

An elastic continuum model for interpretation of seismic behavior of buried pipes as a soil-structure interaction

Un modèle de continuum élastique pour l'interprétation du comportement sismique des conduites enterrés comme une interaction sol-structure

Tohda J.
Osaka City University

Yoshimura H.
Anan National College of Technology

Maruyoshi K.
Dainippon Plastic Co. Ltd.

ABSTRACT: An elastic 2-D continuum model to interpret the seismic behavior of buried pipes as a soil-structure interaction was proposed. The model simulated a condition in which the ground under K_0 -condition was subjected to simple shear due to earthquake. The interface condition between pipe and soil was assumed to be perfectly smooth. A series of 1/30-scaled centrifuge model tests was conducted to verify the proposed model, where normal and tangential earth pressures on, and bending moments of, two model pipes with different flexibilities were precisely measured during 10 cyclic simple shear deformation of model grounds. The proposed model generated results that were consistent with the measured ones, revealing that the proposed model gives a rational interpretation for the seismic soil-pipe interaction, while current design using seismic deformation method based on spring models is misleading.

RÉSUMÉ : Un élastique 2-D modèle de continuum pour interpréter le comportement sismique des conduites enterrés comme une interaction sol-structure a été proposée. Le modèle a simulation simulé une condition dans laquelle le sol sous condition K_0 a été soumis à un cisaillement simple en raison de tremblement de terre. La condition d'interface entre le conduite et le sol était supposé être parfaitement lisse. Une série d'essais sur modèle centrifugeuse en échelle 1/30 a été effectuée afin de vérifier le modèle proposé, où la pression des terres normales et tangentielle sur, les moments de flexion de deux conduites modèles avec différentes flexibilités ont été précisément mesurée pendant 10 déformation de cisaillement cyclique simple des motifs du modèle. Les résultats du modèle proposé qui étaient compatibles avec celles mesurées révélant que le modèle proposé donne une interprétation rationnelle de la sismique interaction sol-conduites, tandis que la conception actuelle en utilisant la méthode déformation sismique basée sur des modèles de printemps n'est pas raisonnable.

KEYWORDS: buried pipe, seismic soil-structure interaction, continuum model, earth pressure, centrifuge model test

1 INTRODUCTION

Two types of models, namely a continuum model and a spring model, to interpret the mechanical behavior (earth pressure and deformation) of buried pipes as a soil-structure interaction were proposed hitherto. However, being their interpretation for the phenomenon different, it often generates confusion in this research field (e.g. Moore 1989). The authors investigated the concentration of earth pressure on rigid pipes and its relaxation on flexible pipes, as well as buckling of thin-walled buried pipes through experimental and analytical researches (Tohda et al. 1986, 1994, 1997 and Tohda 2001), revealing that the continuum model reasonably explains the actual behavior of buried pipes, while the spring model is erroneous.

Current design standards for buried pipes in Japan (e.g. JSWAS 2006) prescribe the application of seismic deformation method based on the spring model to predict the stability of buried pipes against seismic loading. The authors pointed out again that the current design standards prediction for the behavior of buried pipes is different from those observed in dynamic centrifuge model tests (Tohda et al. 2010a). One of the critical differences between the measurements and prediction is the role of tangential earth pressures (τ) acting on the surfaces of buried pipes. τ in the measurement are always almost null, while in the prediction τ is assumed to govern the seismic behavior of buried pipes.

In the present paper, the authors proposed a new elastic 2-D (two-dimensional) continuum model to interpret reasonably the seismic behavior of buried pipes as a soil-structure interaction. Its validity was confirmed through comparison between the analysis and measurement in centrifuge model tests that simu-

lated simple shear deformation of the ground produced by earthquake.

2 PROPOSED MODEL AND ANALYTICAL RESULTS

2.1 Proposed seismic continuum model

Figure 1 shows the proposed 2-D continuum model. The model simulates the condition in which the ground under K_0 -condition is subjected to simple shear due to earthquake. Soil and pipe are assumed as linear elastic bodies. Relative stiffness between soil and pipe ($\kappa = E_s/S_p$) is varied from 0 (pipe as rigid body) to ∞ (a circular cavity exists in the ground). Where, E_s is the Young's modulus of soil; $S_p = E_p t^3 / \{12(1 - \nu_p^2)R^3\}$, the flexural stiffness of the pipe; E_p and ν_p are, respectively, the Young's modulus and Poisson's ratio of the pipe; t is the wall thickness of the pipe, and R , the neutral radius of the pipe. Poisson's ratios of soil (ν_s) are also varied from 0.2 to 0.4.

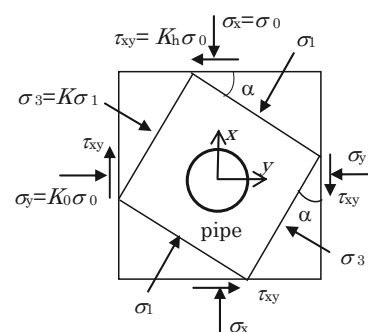


Figure 1. Proposed 2-D seismic continuum model.

A boundary condition at the interface between the pipe and soil is assumed to be perfectly smooth ($\tau=0$). Normal stress $\sigma_x=\sigma_0$ and shear stress $\tau_{xy}=K_h\sigma_0$ are assigned to infinite horizontal planes. Normal stress $\sigma_y=K_0\sigma_0$ and shear stress $\tau_{xy}=K_h\sigma_0$ are assigned to infinite vertical planes. Here, σ_0 corresponds to the vertical stress in the ground produced by soil weight. $K_0(=v_s/(1-v_s))$ is the coefficient of earth pressure at rest, and K_h is the horizontal seismic coefficient.

The maximum and minimum principal stresses (σ_1 and σ_3) and the angle (α) between the horizontal plane and maximum principal plane are expressed by $\sigma_1=[(1+K_0)/2+\{(1-K_0)^2/4+K_h^2\}^{1/2}]\sigma_0$, $\sigma_3=[(1+K_0)/2-\{(1-K_0)^2/4+K_h^2\}^{1/2}]\sigma_0$, and $\sin 2\alpha=K_h/\{(1-K_0)^2/4+K_h^2\}^{1/2}$. When the two coefficients K_0 and K_h are given, $K=\sigma_3/\sigma_1$ and α can be determined. One of the authors derived the solution of a model in which σ_1 and σ_3 act on the infinite horizontal and vertical planes in usual manner of elastic theory using Airy's stress function (Tohda and Mikasa 1986). Thus, the stress and deformation components of the proposed model can be obtained by transforming this solution into the xy axes in Figure 1.

2.2 Analytical results

Figure 2, illustrated in polar coordinates, shows the distributions of normal earth pressure σ/σ_0 acting on the surface of the pipe and bending moment $M/(\sigma_0R^2)$ produced on the pipe wall, analyzed for different κ when $v_s=1/3$ (accordingly $K_0=0.5$) and $K_h=0.5$. Compressive σ are counted as positive. Positive M corresponds to the case where the internal surface of the pipe is under tension. Analyzed τ acting on the surface of the pipe are null.

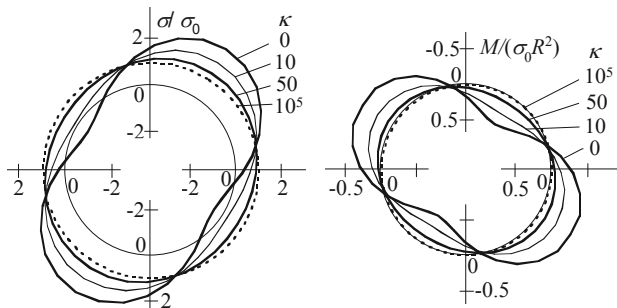


Figure 2. Analyzed σ/σ_0 and $M/(\sigma_0R^2)$ for different κ ($K_h=0.5$, $K_0=0.5$, $v_s=1/3$).

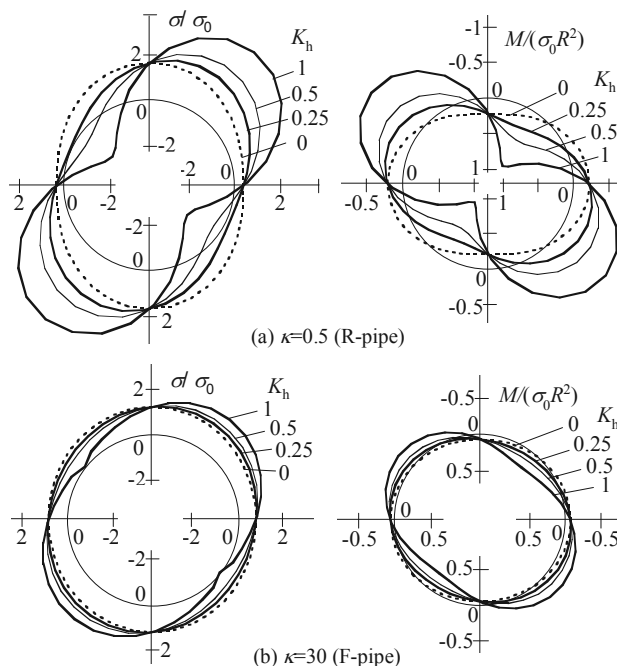


Figure 3. Analyzed σ/σ_0 and $M/(\sigma_0R^2)$ for different K_h ($K_0=0.5$, $v_s=1/3$).

Figure 2 indicates that: 1) The symmetric axes of distributions of both σ/σ_0 and $M/(\sigma_0R^2)$ rotate owing to simple shear of the model, while the rotation angle is unchanged for any κ under the constant K_h condition. 2) The smaller κ is, the greater are the generated maximum values of σ/σ_0 and $M/(\sigma_0R^2)$.

Figure 3 shows σ/σ_0 and $M/(\sigma_0R^2)$ for different K_h when $\kappa=0.5$ and 30, v_s being 1/3 ($K_0=0.5$). As described in Chapter 3, these two κ values are close to those in test cases when R-pipe and F-pipe were buried in a loose dry silica sand ground (S0L-ground). Figure 3 indicates that: 1) In both κ cases, the greater K_h is, the greater are the generated maximum values of both σ/σ_0 and $M/(\sigma_0R^2)$ and the generated value of α . 2) Changes in σ/σ_0 and $M/(\sigma_0R^2)$, as well as their maximum values, are considerably greater when $\kappa=0.5$ than those of $\kappa=30$.

3 CENTRIFUGE MODEL TESTS AND EXPERIMENTAL RESULTS

3.1 Procedure of centrifuge model tests

Two model aluminum pipes, whose dimensions and material properties are shown in Table 1, were used in the tests. They were named as R-pipe and F-pipe according to their flexibilities. Their external diameters (D) and lengths were 90 mm and 148 mm, respectively. Their wall thickness (t) varied from 3.5 mm to 0.95 mm, so that their S_p values are similar to those of the RC-pipe and plastic-pipe (either FRPM-pipe or PVC-pipe) prototypes. The surfaces of the pipes were smoothly finished to simulate those of the prototype pipes. Normal (σ) and tangential (τ) earth pressures acting on the pipe surface at 20 measuring points, as well as bending strains (ϵ) produced on the walls of the pipes at 16 measuring points, were measured. The structure of the model pipes and their instruments were detailed in the literature (Tohda et al. 2010b).

Figure 4 shows the model configuration. The model was scaled to 1/30 of the prototype. The model pipes were buried in model grounds with a cover height (H) of 9 cm or 18 cm ($H/D=1$ and 2) and a distance from the pipe bottom to the ground bottom (H_b) of 15 cm. Thick aluminum plates with hinge systems at the lower ends were placed at the lateral sides of the model grounds. The internal front and back walls of the container, as well as the internal surfaces of the lateral-side plates, were lubricated by means of two sheets of rubber membrane with silicon grease. A sheet of water resistant sand paper (grain size $=0.3-0.7$ mm) was pasted on the bottom of the container.

Two types of soils, dry silica sand (S0) or decomposed granite (S16), were used in the tests. Loose and dense S0-grounds (S0L- and S0D-grounds) were constructed by dry pluviation, and loose S16-ground (S16L-ground) was constructed by compaction. The pluviation or the compaction was carried out in the

Table 1. Dimensions and material properties of model pipes.

Model pipe	D (mm)	t (mm)	E_p (GPa)	ν_p	S_p (MPa)
R-pipe	90	3.5	74	0.33	3.60
F-pipe	90	0.95	74	0.33	0.066

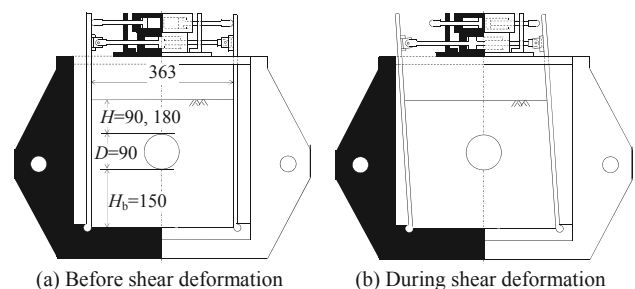


Figure 4. Model configuration (unit: mm).

Table 2. Properties of model grounds.

Ground	G_s	D_{max} (mm)	F_c	U_c	ρ_{dmax} (g/cm ³)	ρ_{dmin} (g/cm ³)	ρ_d (g/cm ³)	w (%)
S0L	2.65	1.4	0	1.75	1.58	1.32	1.43	0
S0D	2.65	1.4	0	1.75	1.58	1.32	1.55	0
S16L	2.71	2.0	16	70	1.92	1.42	1.50	10

direction parallel to the longitudinal axes of the model pipes. The properties of the model grounds are shown in Table 2.

At a centrifugal acceleration field of 30 g (g : gravitational acceleration), the lateral-side plates were rotated by means of the hydraulic cylinder in parallel cyclically ten times, first to the left-side and next to the right-side, until simple shear strain (γ) of the model ground reached 3.2%. Time required for one cycle was 6 minutes. The value of $\gamma=3.2\%$ was determined as an average value of relative shear strains produced between the bottom and top of the pipes that were buried in the different model grounds under resonant conditions due to level-2 seismic motions.

3.2 Experimental results

Marks and thin lines in Figure 5 (R-pipe) and Figure 6 (F-pipe) show σ , τ , and M that were measured at $\gamma=3.2\%$ when the ground was deformed to the left-hand side. The marks and thin lines correspond to the data measured at $N=1, 2, 5$, and 10 (N : number of repetition times for shear). Measured τ acting counterclockwise are counted as positive.

Measured results shown in Figures 5 and 6 indicate that: 1) σ and M increase with an increase in N owing to hardening of soils due to repetitive shear deformation, but they have tendencies to converge when $N \geq 5$. 2) τ are always close to be null. 3) When $H/D=1$, the model grounds with greater K_h tend to generate greater maximum values of σ and M , as well as greater α . 4) Changes in σ and M due to the differences in the test conditions,

as well as the maximum values of σ and M , are considerably greater in R-pipe than in F-pipe.

σ , τ and ε measured for the two model pipes in the present tests were compared with those measured in other dynamic centrifuge model tests (Tohda et al. 2010b), in which the same models as those in the present tests were oscillated 10 times by 1 Hz sinusoidal horizontal acceleration wave with an amplitude of 0.8 g . The comparison showed that: 1) The mechanical behavior of the model pipes obtained in both centrifuge model tests was similar qualitatively. 2) The maximum bending strains (ε_{max}) when $H/D=1$ yielded similar magnitudes in both tests, but ε_{max} when $H/D=2$ were 2 to 3 times greater in the present tests than in the dynamic tests (Ohsugi et al. 2011).

4 COMPARISON BETWEEN ANALYTICAL AND EXPERIMENTAL RESULTS

Input parameters used in the analysis for each experiment were determined as shown in Table 3, as it follows: 1) Total vertical stress in the model ground at the mid-height of the model pipe was assigned to the boundary stress $\sigma_x=\sigma_0$. 2) Values of both E_s at σ_0 and ν_s (constant regardless of σ_0) were determined from K_0 -compression tests using a rectangular box. 3) K_0 value was obtained from ν_s through $K_0 = \nu_s / (1 - \nu_s)$. 4) τ_{xy} and K_h values were obtained from E_s , ν_s and $\gamma=3.2\%$ through $\tau_{xy}=G\gamma = E_s\gamma / \{2(1+\nu_s)\} = K_h\sigma_0$. Table 3 indicates that the difference in K_h

Table 3. Input parameters used in the analysis for each experiment.

Test condition		σ_0	ν_s	E_s	K_0	τ_{xy}	K_h
Ground	H/D	(kPa)		(kPa)		(kPa)	
S0L	1	57	0.37	2050	0.59	24	0.42
S0L	2	95	0.37	2880	0.59	34	0.35
S16L	1	66	0.33	830	0.49	10	0.15
S0D	1	62	0.35	4570	0.54	54	0.88

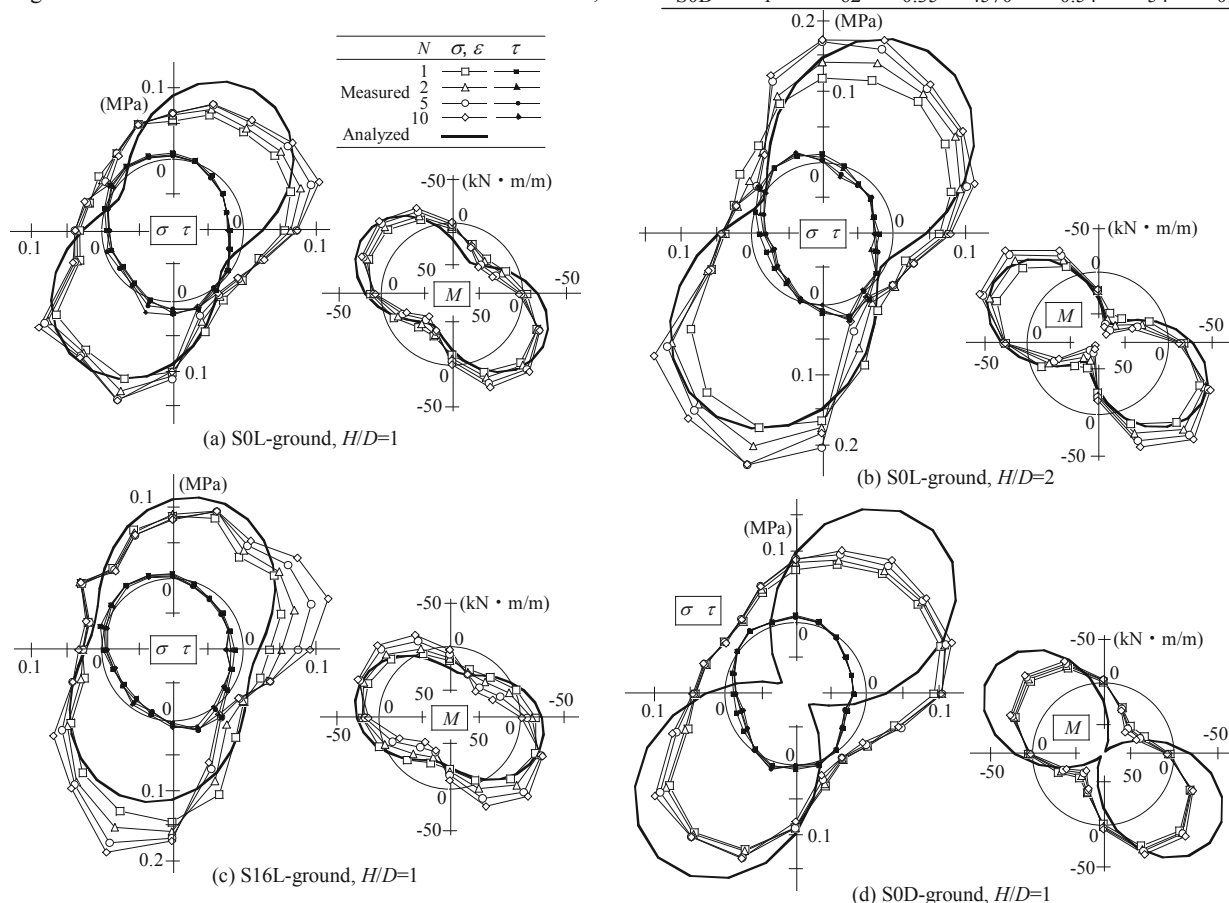


Figure 5. Comparison between experimental and analytical results (R-pipe).

for different types of the model grounds is remarkable, while the difference in K_0 values is not so high.

Thick lines in Figure 5 (R-pipe) and Figure 6 (F-pipe) show the analytical results. The analytical τ are null. Comparison between analytical and experimental results indicates that the analytical results in Figures 5 and 6, as well as those shown in Figure 3, are consistent with the experimental results except for exceptional cases. It should be noted that the measured τ in the experiment are always close to be null, which conformed to $\tau=0$ in the analysis. However, the current design standards using the seismic deformation method based on the spring model assume that τ acting on the pipe surface govern the seismic behavior of buried pipes. This contradicts with the results obtained in the experiment and analysis, revealing that the current seismic design standards are misleading.

One of the analyzed cases being inconsistent with the experiment is the case when R-pipe was buried in S0D-ground. There are two areas in which the analyzed σ are negative (tension). As soil cannot resist tension, separation between the pipe and soil must have occurred in the experiment. This separation must have generated redistribution of earth pressure, resulting in smaller σ and M in the experiment than in the analysis. This interpretation was validated by a FEM analysis in which the separation at the pipe-soil interface was considered.

Another exceptional point of inconsistency between the analysis and experiment is the specific concentration of σ measured at two measuring points 18° or 36° apart from the top and bottom of F-pipe (cf. Figure 6). Its magnitude increases with the increase in N in any case. The concentration points of σ exactly reversed when the ground was deformed to the right-hand side. The analysis showed that the soil elements close to the surface of F-pipe at the concentration points of σ were subjected to compressive mean stresses, whose magnitudes were around two times greater than those in R-pipe. On the other hand, the magnitudes of deviator stresses at the corresponding points were similar in F-pipe and R-pipe. It was supposed, therefore, that compression of the soil close to the concentration points of σ in F-pipe must have strengthened the rigidity of the soil irreversibly during the iterative simple shear in the tests, resulting in the specific concentration of σ on F-pipe.

5 CONCLUSIONS

The validity of the proposed continuum model for interpretation of the seismic behavior of buried pipes as soil-pipe interaction was confirmed by experiment. It can be concluded, therefore, that a basic theory for seismic design of buried pipes, instead of current seismic design based on problematical spring models, was provided by this study.

6 REFERENCES

- Moore I.D. 1989. Elastic buckling of buried flexible tubes – A review of theory and experiment. *Journal of Geotechnical Engg., ASCE*, 115(3), 340-358.
- Tohda J. and Mikasa M. 1986. A study of earth pressure acting on buried pipes through theory of elasticity. *Journal of JSCE* 376(III-6), 181-190.
- Tohda J., Li L., and Yoshimura H. 1994. Analysis of the factors in earth pressure and deformation of buried flexible pipes through centrifuge model tests, *ASTM STP1222 Buried Pipe Technology*, 180-194.
- Tohda J., Yoshimura H., and Li L. 1997. Mechanical behavior and design of buried pipes as a soil-structure interaction, *Proc. of the 14th ISSMFE*, 1049-1052.
- Tohda J. 2001. A study of buckling behavior of buried pipes through theory of elasticity. *Journal of JGS (Tsuchi-to-kiso)* 49(4), 19-22.
- JSWAS (Japanese Sewage Works Association). 2006. Earthquake-resistant measures guidelines and commentary of sewer facilities.
- Tohda J., Yoshimura H., Inoue Y., and Mukaichi H. 2010a. Centrifuge model tests and analysis on seismic behavior of sewer culverts. *Journal of JGS (Tsuchi-to-kiso)* 58(2), 18-21.
- Tohda J., Yoshimura H., Ohsugi A., Nakanishi K., Ko H.Y., and Wallen R.B. 2010b. Centrifuge model tests on dynamic response of sewer trunk culverts, *International Conference on Physical Modeling in Geotechnics (ICPMG 2010)*, 651-656.
- Ohsugi A., Nakanishi K., Tohda J., Maruyoshi K., Yoshimura H., and Inoue Y. 2011. Stability against seismic loading, of sewer trunk culverts severely deteriorated after renovated by lining methods with discrete pipes and spirally wound pipes, *Proc. of the 46th Annual Conference on Geotechnical Engineering, JGS*, 1459-1460.

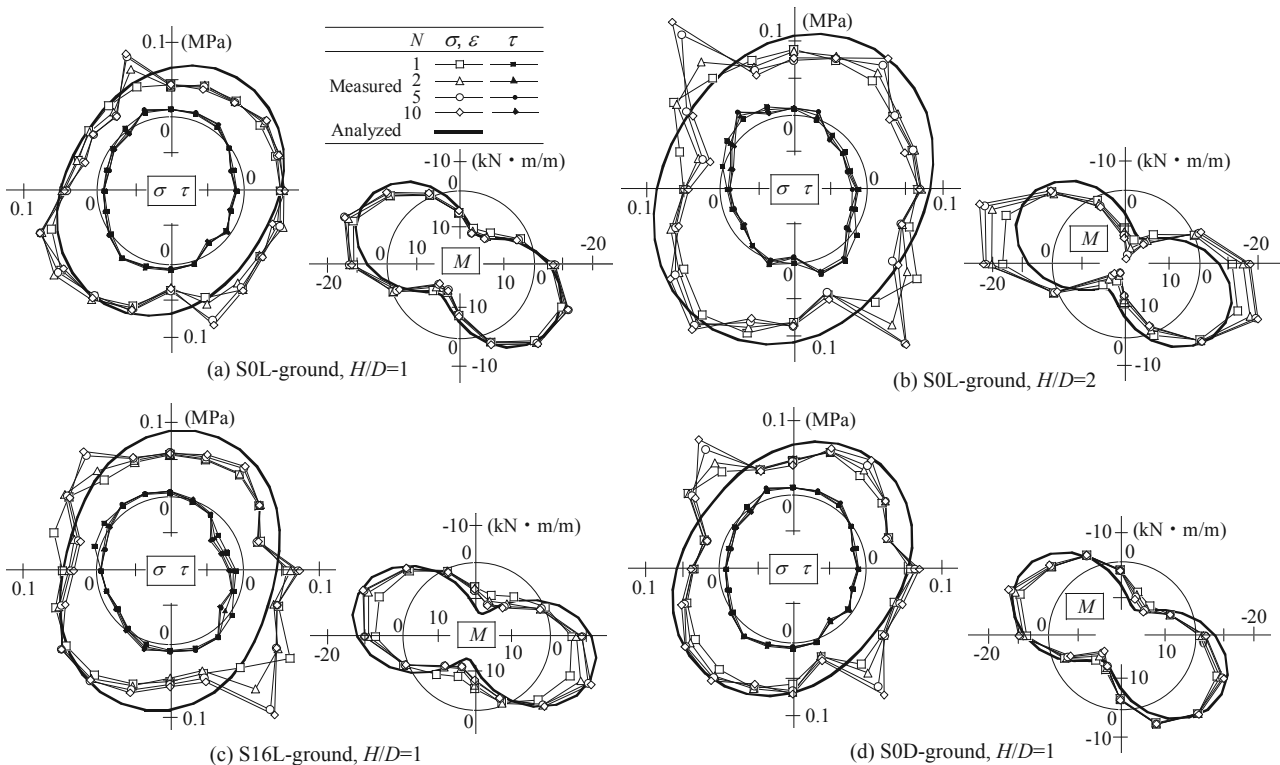


Figure 6. Comparison between experimental and analytical results (F-pipe).